

## Mössbauer-spectroscopy study of amorphous Fe-Ge alloys

H. H. Hamdeh and M. R. Al-Hilali

*Department of Physics, Wichita State University, Wichita, Kansas 67208*

N. S. Dixon and L. S. Fritz

*Department of Physics, Franklin and Marshall College, Lancaster, Pennsylvania 17604*

(Received 25 March 1991)

A Mössbauer-spectroscopy study of amorphous  $\text{Fe}_x\text{Ge}_{1-x}$ , with  $0.11 < x < 0.72$ , was performed to measure the hyperfine-field parameters at 22 and 295 K. The distributions of quadrupole splitting suggest that for  $x < 0.2$ , the structure of the alloys is homogeneous and Fe atoms probably occupy the interstices of the Ge tetrahedral structure. For concentrations of  $x > 0.4$ , however, hyperfine-field parameters seem to indicate that the alloys contain a mixture of short-range-order phases, with the average hyperfine magnetic field rising sharply with concentration. The resulting analysis of isomer shift, in terms of the model of Miedema and Van der Woude [*Physica B* **100**, 145 (1980)], shows the Fe magnetic moment to be strongly influenced by hybridization and intra-atomic charge redistribution.

### I. INTRODUCTION

Amorphous Fe-Ge alloys undergo two important transitions as the composition is varied. The metallic properties start at 15–25 at. % Fe,<sup>1,2</sup> while the ferromagnetic properties start at about 40 at. % Fe.<sup>3,4</sup> Change in topological and chemical short-range order (SRO) with composition is still a challenging problem, especially at the two transition compositions.

Two models have been proposed to describe how Fe atoms are situated in the random tetrahedral network, characteristic of pure amorphous Ge, in Ge rich Fe-Ge alloys. One model<sup>5</sup> suggests that on introducing Fe in the Ge matrix for low concentration of Fe, the Fe atoms go into substitutional positions without significantly disturbing the tetrahedral stacking. But on further increasing the Fe content, the Ge tetrahedral structure is progressively destroyed and the structure becomes more like that of packed hard spheres. A second model<sup>6</sup> suggests that Fe atoms occupy the interstices of the Ge tetrahedral structure up to the limit of 19 at. % Fe, when the network is completely filled.

On the other hand, several models have been proposed to explain the absence of any magnetic ordering at any temperature for concentrations below a critical value  $x_c$ . One model suggests that Fe bears a substantial magnetic moment below  $x_c$ , but  $x_c$  is a percolation threshold.<sup>7</sup> Other models advocate the disappearance of the Fe magnetic moment below  $x_c$ . However, two distinct mechanisms, by which the magnetic moment of Fe vanishes, are proposed. One mechanism<sup>8</sup> is a charge-transfer mechanism, where  $4p$  electrons of Ge are transferred to the Fe  $3d$  band, which leads to a more complete  $3d$  band filling. The second one<sup>9</sup> is a broadening mechanism, where the Fe  $3d$  band hybridizes with the Ge  $sp$  levels, which leads to a spin-degenerate Fe  $3d$  band. According to these models, the appearance of the Fe magnetic moment is linked to the average number of Fe atom nearest neighbors. Most recently, the local density of the Fe  $3d$  elec-

trons in the Fe-Ge system was directly measured by electron energy-loss spectroscopy (EELS).<sup>10,11</sup> The results were found to suggest hybridization as the cause for the decrease in the Fe magnetic moment as the Ge content is increased. However, charge transfer was not ruled out in the similar Fe-Si system.

Recent extended x-ray-absorption fine structure (EXAFS) and x-ray appearance near-edge structure (XANES) measurements<sup>12</sup> on sputtered samples have shown that the Fe-Ge system remains homogeneous in the concentration range below 33 at. % Fe, which includes the semiconductor-to-metallic transition, and separates into phases above 37 at. % Fe, which includes the magnetic transition. In the present study, the hyperfine parameters of amorphous  $\text{Fe}_x\text{Ge}_{1-x}$ , with  $0.11 < x < 0.72$ , are measured at room temperature and at 22 K. Analyses of quadrupole splitting (QS) and hyperfine magnetic-field (HMF) distributions, which are presented in Sec. III and Sec. IV, respectively, complement the EXAFS and XANES investigation of structural properties. In addition to the HMF data, isomer shift data, which are presented in Sec. V, provide valuable information about the magnetic properties.

### II. EXPERIMENT AND DATA ANALYSIS

Amorphous samples of  $\text{Fe}_x\text{Ge}_{1-x}$  with  $0.11 < x < 0.72$  were prepared by R. D. Lorentz at Stanford University by cosputtering from pure Fe and Ge targets onto a rapidly rotating, uncooled table holding the sample substrates. The rotation of the table ensured compositional homogeneity over a large scale. Thin Kapton films were used as substrates. During deposition, substrate temperatures rose above that of the table because they were not thermally connected. Sample composition was determined by Auger electron spectroscopy which was conducted over different parts of the sample. A continuous x-ray-diffraction scan was used to check for any evidence of crystallization. Further details of deposition and sam-

ple analyses are reported elsewhere.<sup>12</sup>

Mössbauer spectra were obtained in a transmission geometry with a conventional constant-acceleration spectrometer. The average film thickness was about 1  $\mu\text{m}$ . Each specimen used in this work consisted of a few 1-cm<sup>2</sup> layers stacked together, hence no thickness correction was necessary. A radiation source of 50-mCi <sup>57</sup>Co in a Rh matrix was used for all measurements. Mössbauer spectra were obtained at 22 K and room temperature. In amorphous Fe-Ge alloys, the quadrupole-splitting, hyperfine-magnetic-field, and isomer-shift distributions result in broadening of all Mössbauer lines with respect to those of pure Fe. The distributions of the quadrupole splitting and the hyperfine magnetic field were obtained by two methods. In these methods, the isomer-shift distribution was neglected and only average isomer-shift values were obtained. In the first, the following distribution was considered:

$$P(X) = \sum_{i=1}^n A_i \exp \left[ -\frac{1}{2} \left( \frac{X - X_{0i}}{\sigma_i} \right)^2 \right],$$

where  $x$  is QS or HMF,  $A_i$  is a constant; ( $\sum A_i = 1$ ),  $\sigma_i$  is related to the width of the  $i$ th Gaussian distribution. A maximum of  $n = 3$  was used. The QS distribution was convolved with a doublet of Lorentzian lines and the HMF was convolved with a sextet of Lorentzian lines characteristic of a pure Fe spectrum. In addition to the average isomer shift of each Gaussian distribution, the parameters  $A_i$ ,  $x_{0i}$ , and  $\sigma_i$  were all freely adjusted in a least-squares fit to the experimental data. In the second method, we employed the analysis procedure of Le Caër and Dubois.<sup>13</sup> This method provides both discrete and continuous distributions of the hyperfine-field parameters directly, and no prior knowledge of the distribution shapes is required. The results of the mean and the variance of the distributions of the two methods are in full agreement. It is worth noting here that there may be an added broadening to the HMF distribution from the possibility of random orientation of the electric-field-gradient axes relative to the magnetic direction.

### III. QUADRUPOLE SPLITTING

All the Mössbauer spectra of amorphous Fe<sub>x</sub>Ge<sub>1-x</sub> at room temperature with  $x = 0.11, 0.18, 0.27, 0.43, 0.45,$  and  $0.49$  exhibit only a quadrupole doublet, while at 22 K a resolved doublet is seen only for the spectra with  $x \leq 0.27$ . In the absence of any magnetic order, the measured distributions of the QS are rather accurate within experimental errors and show no significant dependence on temperature. The mean and the variance of the QS distributions as a function of  $x$  are shown in Fig. 1 for the spectra at room temperature. With the exception of  $x = 0.52$  (Curie temperature is around room temperature), the mean QS decreases continuously with increasing Fe concentration. As a measure of the electric field gradient (EFG) at the <sup>57</sup>Fe nucleus, which is determined by the local symmetry at the Fe site, QS size is strongly related to the near-neighbor configuration. Consequently, the results suggest simply that on the average the local symmetry shows a steady increase throughout the

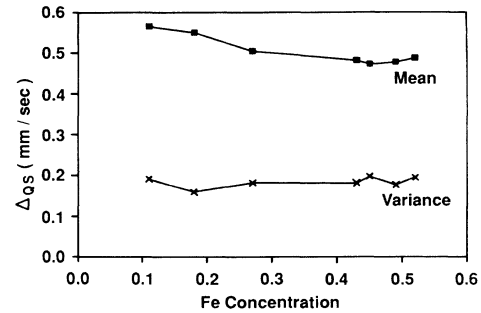


FIG. 1. Mean (■) and the square root of the variance (×) of the <sup>57</sup>Fe QS distribution  $\Delta_{QS}$  obtained from spectra measured at room temperature vs Fe concentration.

specified concentration range of Fe. On the other hand, the variances show that the width of the QS distribution is nearly constant. On further analysis of the distributions which are presented in Fig. 2, two important observations can be made. (1) The QS distributions of the alloys at  $x = 0.11$  and  $0.18$  show a peak that is centered around  $\Delta_{QS} = 0$  mm/sec, which results from anisotropy that exists in these two alloys. Theoretical calculations of these distributions yield the above results, with the assumption that the intensities of the two Mössbauer lines are equal; but this is not supported by the experimental spectra of the two alloys. To check for the EFG anisotropy, the samples were rotated in order to change the angle between the  $\gamma$  ray direction and the plane of the film. The corresponding change in the relative intensities of the lines matched roughly the theoretical predictions for thin films and also suggests a positive sign for the QS. (2) Although the mean and the variance of the distributions decrease with increasing Fe concentration from  $x = 0.11$  to  $0.18$ , the center of the main peak ( $\Delta_{QS} = 0.52$  mm/sec) does not change. Therefore, it is inappropriate to consider that the local symmetry increases homogeneously throughout the alloys in this concentration range. The most likely explanation for these two observed behaviors is that the Fe atoms occupy randomly the interstitial sites of the Ge tetrahedral network. The  $\Delta_{QS} = 0.52$  mm/sec peak represents those Fe atoms with the nearest-neighbor interstitial sites completely filled; further addition of Fe atoms simply fills the remaining empty sites, thus narrowing the width of the distribution and leaving the center of the peak in place. Also, from point symmetry one knows that the EFG at the interstitial hexagonal sites of a random tetrahedral structure has a large (111) axial symmetry, while the EFG axes are expected to be randomly oriented in a dense random packing of neighbors. Therefore, it is less likely for anisotropy to exist in the latter system than in the first one.

In addition, the QS distribution of the alloy at  $x = 0.11$  also features a small peak that is centered around  $\Delta_{QS} = 1.1$  mm/sec. By comparing this peak to the values<sup>14</sup> of the QS of amorphous Fe-Ge alloys in the dilute limit, we identify this high QS peak as the QS of individual <sup>57</sup>Fe atoms situated on sites within regions of pure Ge environment. While the main peak of the distribu-

tions of the alloys with  $x=0.11$  and  $0.18$  resembles a Gaussian distribution, the distribution of the alloy at  $x=0.27$  is a single peak centered at  $\Delta_{QS}=0.52$  mm/sec with negative skewness. This skewness is evidence of the growth of Fe sites with increased symmetry as the Fe content is increased from 18 to 27%. The center of the peak has shifted down to  $\Delta_{QS}=0.48$  mm/sec for the alloys with  $x=0.43, 0.49,$  and  $0.52$ , while the QS distribution of the alloy with  $x=0.45$  has split into two peaks centered around  $\Delta_{QS}=0.30$  mm/sec and  $\Delta_{QS}=0.55$  mm/sec. All this suggests that major structural changes are taking place at  $x > 0.43$ , with the possibility of more than one local order developing.

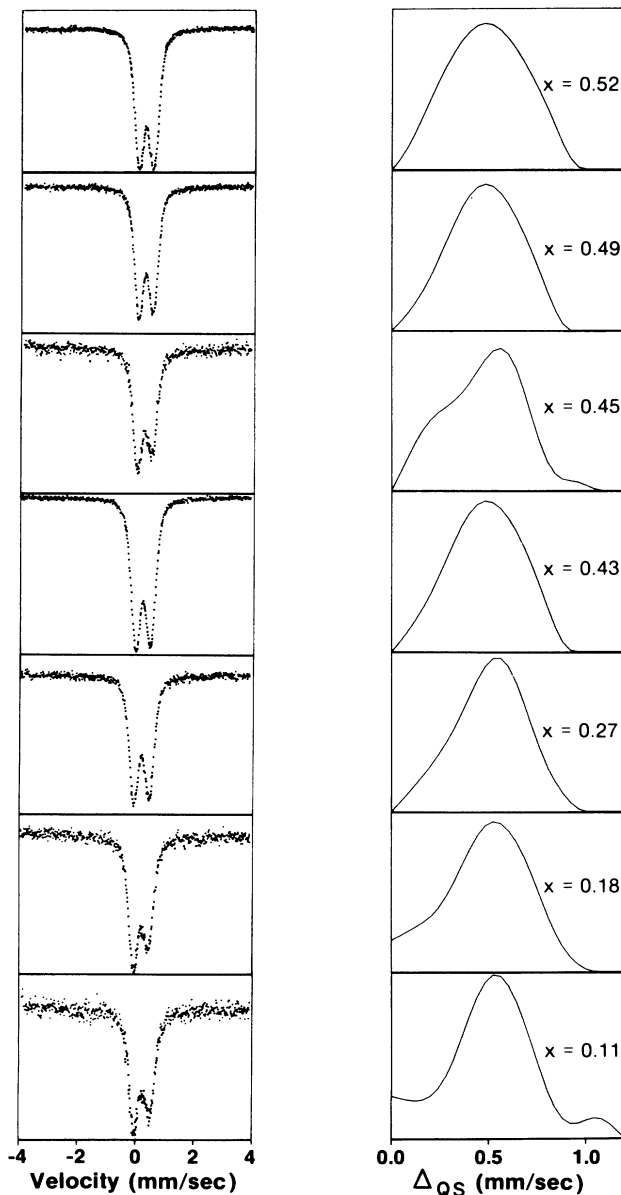


FIG. 2. Left: Mössbauer spectra measured at room temperature from sputtered Fe-Ge. Right:  $^{57}\text{Fe}$  QS distributions  $\Delta_{QS}$  obtained from the spectra on the left by the method of Le Caër.

We were unable to identify accurately the possible phases by comparing our QS data to those of the various Fe-Ge intermetallics for two reasons. First, the nature of the substrates prevented us from performing serious annealing of the samples to better resolve the peaks. Second, most of the reported QS data<sup>15-21</sup> of the Fe-Ge binary is measured below  $T_c$  and the relative orientation between the EFG axes and the direction of the magnetic field is neglected. This is probably the reason for the unusual discrepancy in the published data.

#### IV. HYPERFINE MAGNETIC FIELD

The Mössbauer spectra taken at 22 K from alloys with  $x > 0.43$  clearly indicate the presence of magnetic order in these alloys. The spectra from alloys with  $x \leq 0.52$  are considered to contain a distribution of six line patterns which originate from magnetically ordered  $^{57}\text{Fe}$  atoms, and a distribution of quadrupole doublets. The two independent distributions and their concentrations are obtained by employing the Le Caër and Dubois method. The Mössbauer spectra and the  $^{57}\text{Fe}$  HMF distributions obtained from them are presented in Fig. 3. Also presented is the HMF of various Fe-Ge intermetallics and pure Fe for comparison.

The broad HMF distribution at the  $^{57}\text{Fe}$  changes significantly with the Fe concentration and features more than one peak. The first peak centered at about 50 kG is usually characterized as the nonmagnetic or paramagnetic peak; however, Fe atoms of persisting short-range magnetic order are also included in this peak. As expected, the intensity of this peak changes rapidly with temperature. The other peaks are considered to correspond to different  $^{57}\text{Fe}$  sites, and the intensity of each peak represents approximately the probability of each environment. It is clear that the sample at  $x=0.72$  contains two SRO phases which can be described as the SRO of the crystalline compounds of  $\text{FeGe}_2$  and  $\text{Fe}_3\text{Ge}$ . To quantify the intensities of the two environments, the two peaks in the HMF distribution were fit to a set of two Gaussian functions. The high Fe concentration phase makes up about 92% of the alloy. We were also able to find the area under the hexagonal Fe-Ge peak of the sample at  $x=0.52$  to be 60% of the HMF distribution; however, this phase makes up only 53% of the alloy since 11% of  $^{57}\text{Fe}$  atoms are not magnetically ordered. Because of the strong overlap among the peaks in the HMF distributions of the other samples, it was not possible to quantify accurately their intensities. However, it appears generally that the major amorphous phase that makes up an alloy is similar to the crystalline Fe-Ge binary with composition close to that of the alloy. The HMF distributions of the two highest Fe concentration alloys measured at 22 K differ from those taken at room temperature (see Fig. 3). This may be attributed to the difference in temperature dependence of the HMF of the various phases.

It has been shown in crystalline compounds of Fe-Ge, that the HMF is roughly proportional to the magnetic moment of Fe as determined by Mössbauer measurements and neutron-diffraction or magnetization measurements. In order to make a meaningful comparison be-

tween our HMF data and magnetization data, we present the mean  $^{57}\text{Fe}$  HMF vs Fe concentration in Fig. 4. Our data are in good agreement with the magnetization data of Suran, Daver, and Bruyere<sup>4</sup> and confirm the widely observed critical concentration  $x_c = 0.4$  below which magnetization is absent down to 4.2 K.

Upon obtaining the HMF distributions, we assumed the spatially averaged values of the QS to be equal to zero in the presence of long-range magnetic order. This is indeed the case as shown by the spectra of the two highest Fe concentrations. These spectra also show that the relative intensities of the Mössbauer lines closely follow the expected relation 3:1. At room temperature the

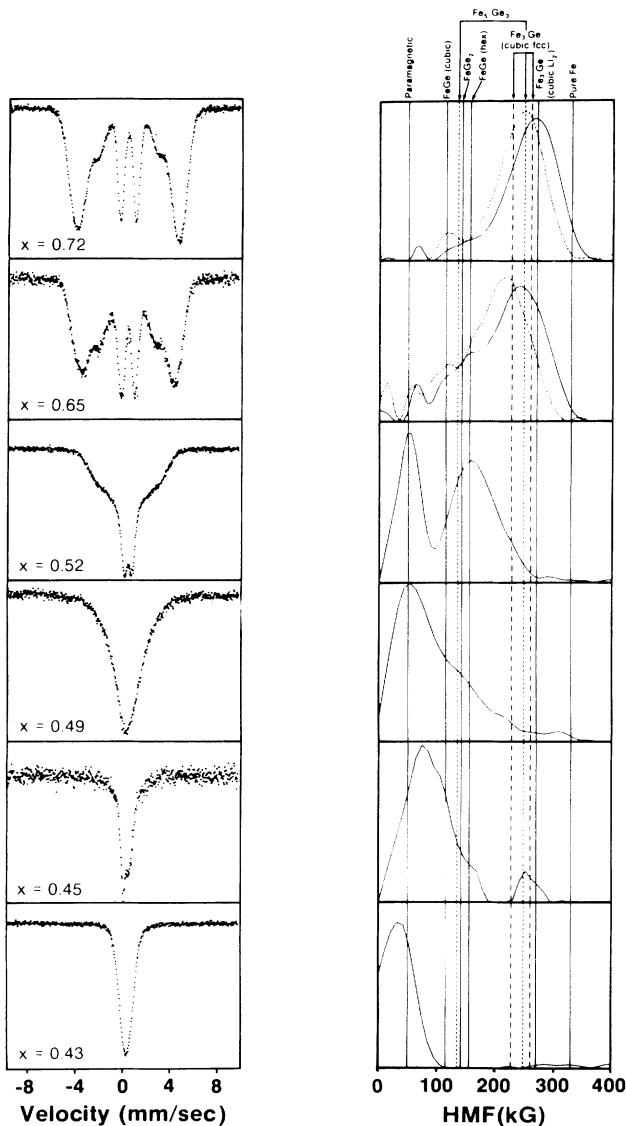


FIG. 3. Left: Mössbauer spectra measured at 22 K from sputtered Fe-Ge. Right:  $^{57}\text{Fe}$  HMF distributions obtained by the method of Le Caër. The solid curves were obtained from the spectra on the left; the dotted curves were obtained from spectra measured at room temperature. The vertical lines are the HMF values of various crystalline Fe-Ge (Refs. 15–21) alloys and pure Fe.

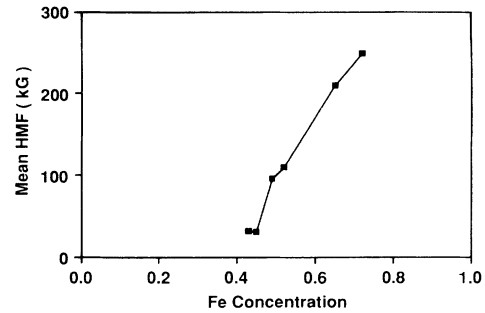


FIG. 4. Mean HMF of the  $^{57}\text{Fe}$  distribution obtained from spectra measured at 22 K vs Fe concentration.

intensity of the second line was close to  $b = 2$ , suggesting that the axis of magnetization is randomly oriented in all directions. At 22 K the value of  $b$  decreased to 0.36, suggesting that the axis of magnetization had rotated out of the plane of the film. This temperature-induced anisotropy could be expected due to the difference in thermal expansion between sample and substrates. The substrates contracted faster thus applying a contractive pressure along the plane of the film. For a positively magnetostrictive alloy, this pressure causes the plane's component of the axis of magnetization to tilt out of the plane.

## V. ISOMER SHIFT

The isomer shifts of the various Fe-Ge intermetallics are reported to be between 0.25 and 0.5 mm/sec. Because of the large overlapping among the different amorphous phases in the present alloys, accurate values of the isomer shift of each phase were difficult to obtain from the measured spectra. The mean values of isomer shift at 22 K (relative to pure Fe at 22 K) of amorphous  $\text{Fe}_x\text{Ge}_{1-x}$  as a function of  $x$  are presented in Fig. 5. These data are similar to that of Massenot and Daver.<sup>22</sup>

Although isomer shift is a measure of charge density of  $s$ -like electrons at the  $^{57}\text{Fe}$  nucleus, the observed variation with Fe concentration is the result of direct changes in the number of  $4s$  and  $3d$  electrons or their wave functions. The core electrons of  $1s$ ,  $2s$ , and  $3s$  are sensitive to the surrounding atoms through their interaction with the

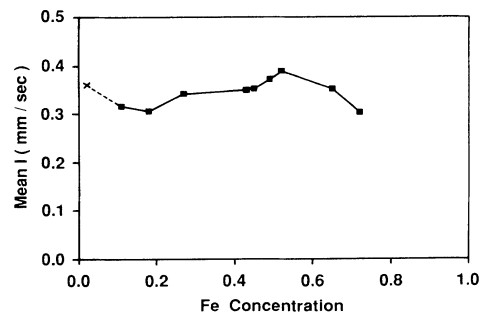


FIG. 5. Mean  $^{57}\text{Fe}$  isomer shift (relative to pure Fe) at 22 K vs Fe concentration. The leftmost point ( $\times$ ) is taken from Ref. 14.

$^{57}\text{Fe}$  3d electrons. In amorphous Fe-Ge alloys, the isomer shift and thus the Fe electronic structure is influenced by the nature of the surrounding atoms as well as by the volume that the Fe atom occupies. Although a direct relation between isomer shift and electronic configuration does exist, no such relation has been formulated yet. Fateseas<sup>23</sup> proposed an isomer shift-electronic configuration diagram, where theoretical charge densities of various configurations of Fe atoms were plotted against the charge of the 4s electrons. However, to resort to this diagram for the interpretation of the experimental isomer-shift data requires a prior knowledge of the total charge of the valence states.

In order to relate the isomer shift at the  $^{57}\text{Fe}$  nucleus to the Fe electronic structure in the dilute  $\text{Fe}_x\text{Ge}_{1-x}$  system, we employed a model that was proposed by Miedema and Van der Woude.<sup>24</sup> This model can be expressed in terms of two main parameters, introduced in describing the heats of formation of alloys. The first is charge transfer from or to an atomic site due to the difference in electronegativity ( $\Delta\Phi$ ) of dissimilar atoms, the second is the discontinuity in charge density which exists at the boundary between dissimilar atoms. The last parameter adds to the isomer shift, usually but not always through intra-atomic conversion in order for the electron density to be continuous at the boundary. To account for hybridization effects of the 3d band of Fe with the sp bands of Ge, a third factor must be added. Applying the model to amorphous  $\text{Fe}_x\text{Ge}_{1-x}$ , the isomer shift in the dilute limit can be described by

$$I_0 = P(\Phi_{\text{Ge}} - \Phi_{\text{Fe}}) + Q \frac{(n_{\text{WS}}^{\text{Ge}} - n_{\text{WS}}^{\text{Fe}})}{n_{\text{WS}}^{\text{Fe}}} + R,$$

where  $I_0$  represents the isomer shift in the dilute limit, where Fe atoms are completely surrounded by Ge neighbors,  $n_{\text{WS}}^{\text{Fe}}$  and  $n_{\text{WS}}^{\text{Ge}}$  are the electron densities at the boundaries of the two original pure atomic Wigner-Seitz cells, and  $R$  is the hybridization factor.

The values of the constant  $P = 0.75$  and  $Q = -1.65$  are calculated by van der Kraan and Buschow,<sup>25</sup> after plotting experimental values of  $I_0/\Delta\Phi$  vs  $(\Delta n_{\text{WS}}/n_{\text{WS}}^{\text{Fe}})/\Delta\Phi$  for Fe-based alloys where hybridization effects are absent. By substituting the electronegativity values of  $\Phi_{\text{Ge}} = 4.93$  V and  $\Phi_{\text{Fe}} = 4.55$  V, and the electron density values  $n_{\text{WS}}^{\text{Fe}} = 5.55$  and  $n_{\text{WS}}^{\text{Ge}} = 2.75$  as listed by Miedema and Van der Woude,<sup>24</sup> the first two terms are found to be equal to  $-0.285$  mm/sec and  $0.886$  mm/sec, respectively. For the calculated  $I_0$  to agree with the average experimental value of  $0.32$  (see Fig. 5), the hybridization term must add a value of  $-0.28$  mm/sec. If one considers that the transferred charge from Ge goes to the Fe 4s band, and with  $\partial I/\partial n_{4s} = -2.0$  (mm/sec)/electron, as estimated by Walker, Wertheim, and Jaccarino,<sup>26</sup> an isomer shift of  $-0.28$  mm/sec corresponds to a charge transfer of  $0.14$  electron. The second term in the isomer-shift equation is directly related to the filling of the Fe 3d band. It is characterized by the intra-atomic  $4s \rightarrow 3d$  charge conversion. With  $\partial I/\partial n_{3d} = 0.2$  (mm/sec)/electron as obtained by Hamdeh, Fultz, and Pearson,<sup>27</sup> this term corresponds

to  $4s \rightarrow 3d$  charge conversion of  $0.40$  electron. The hybridization's main effect is to broaden the 3d band of Fe and possibly to increase the Ge sp charge density at the Fe site. However, the negative contribution to the isomer shift by the hybridization term indicates an increase in s-like electron density at the Fe nucleus as a consequence of the 3d band expansion. The hybridization effect on isomer shift is equivalent to the reduction of 3d electrons by  $1.4$  electrons. From the preceding analysis the electron configuration of metallic Fe undergoes the following changes upon alloying with Ge in the dilute limit: The valence electrons increase by  $0.14$  electron as a result of charge transfer from Ge atoms, the 4s electrons decrease by  $0.26$  electron, while the 3d electrons increase by  $0.4$  electron.

According to this model, the contact surface plays an important role as the boundary conditions change when the atomic cells transfer from their elemental environment to the alloy. The larger the contact surface between Fe and Ge atoms, the larger is the isomer shift. Consequently, the mean values of the isomer shift should decrease as the contact surface concentration of Ge ( $C_s^{\text{Ge}}$ ) decreases with Fe concentration if the structure of the amorphous alloys is homogeneous. This appears to be the case only in the low Fe concentration range as shown by Fig. 5. At higher Fe concentration when SRO phases start to develop, the contact surface between an Fe atom and Ge atoms depends more on the type of the evolving SRO, rather than on Fe concentration. The observed variation of the experimental mean values of the isomer shift may suggest such development of SRO phases.

## VI. CONCLUSION

The QS data indicate a continuous increase in the average coordination number with Fe concentration. In the concentration range  $x < 0.20$ , Fe atoms seem to occupy the interstices of the random tetrahedral network of Ge. For  $x > 0.4$ , all hyperfine-field parameters suggest the presence of significant SRO. The alloys were found to contain amorphous phases with local order which resembles the chemical SRO of some of the Fe-Ge intermetallics.

From the concentration dependence of the average HMF at  $22$  K, we were able to estimate the value of  $x_c$  to be around  $0.40$ . It appears that  $x_c$  coincides with the lower limit of the concentration range when phases start to form. This may suggest an association between the nonmagnetic-to-magnetic transition and the evolution of SRO. In this case, existing theories explaining this transition need to be reconsidered because they ignored any correlation between the occupancies of the near-neighbor shells of the Fe atom. Our QS data along with other structural studies rule out the percolation limit to be the cause of absence of magnetism below  $x_c$ . The percolation theories predict  $x_c$  to be  $0.42$  if the coordination number is equal to  $4$ , which is inconsistent with our data. Therefore, the absence of magnetism is the result of the disappearance of Fe magnetic moments below  $x_c$ . The model

of Miedema and Van der Woude which includes charge transfer,  $4s \rightarrow 3d$  charge conversion, and hybridization was used to analyze the isomer shift. Together with HFM, the resulting analysis shows the Fe magnetic moment to be mainly influenced by hybridization and intratomic charge redistribution.

#### ACKNOWLEDGMENTS

This work was supported by the College of Liberal Arts and Sciences and by the University Research Grant at The Wichita State University. The authors thank Dr. R. D. Lorentz for providing the samples.

- 
- <sup>1</sup>C. L. Tsai (private communication).
- <sup>2</sup>H. Daver, O. Massenet, and B. Chakraverty, *Proceedings of the Fifth International Conference on Amorphous and Liquid Semiconductors*, Garmisch Partenkirchen, 1973 (Taylor and Francis, London, 1974), p. 1053.
- <sup>3</sup>P. Mangin, M. Piecuch, G. Marchal, and C. Janot, *J. Phys. F* **8**, 2085 (1978).
- <sup>4</sup>G. Suran, H. Daver, and J. C. Bruyere, in *Magnetism and Magnetic Materials—1975 (Philadelphia)*, Proceedings of the 21st Annual Conference on Magnetism and Magnetic Materials, edited by J. J. Bocker, G. H. Lander, and J. J. Rhyne, AIP Conf. Proc. No. 29 (AIP, New York, 1976), p. 162.
- <sup>5</sup>O. Massenet, H. Daver, and J. Geneste, *J. Phys. (Paris) Colloq.* **35**, C4-279 (1974).
- <sup>6</sup>Mihai A. Popescu, *J. Non-Cryst. Solids* **56**, 273 (1983).
- <sup>7</sup>Peter Terzieff, Kenneth Lee, and Neil Heiman, *J. Appl. Phys.* **50**, 1031 (1979).
- <sup>8</sup>E. P. Wohlfarth, *IEEE Trans. Magn.* **14**, 933 (1978).
- <sup>9</sup>E. F. Luborsky, S. L. Walter, and E. P. Wohlfarth, *J. Phys. F* **10**, 959 (1980).
- <sup>10</sup>T. I. Morrison, M. B. Brodsky, N. J. Zaluzec, and L. R. Sill, *Phys. Rev. B* **32**, 3107 (1985).
- <sup>11</sup>T. I. Morrison, M. B. Brodsky, and N. J. Zaluzec, *J. Phys. (Paris) Colloq.* **47**, C8-1073 (1986).
- <sup>12</sup>R. D. Lorentz, dissertation, Stanford University, 1986.
- <sup>13</sup>G. Le Caër and J. M. Dubois, *J. Phys. E* **12**, 1087 (1979).
- <sup>14</sup>J. A. Sawicki and B. D. Sawicka, *Phys. Status Solidi B* **80**, K41 (1977).
- <sup>15</sup>J. B. Forsyth, C. E. Johnson, and P. J. Brown, *Philos. Mag.* **10**, 713 (1964).
- <sup>16</sup>R. Wappling, L. Häggström, and E. Karlsson, *Phys. Scr.* **2**, 233 (1970).
- <sup>17</sup>Lennart Häggström, Tore Ericsson, Roger Wäppling, and Erik Karlsson, *Phys. Scr.* **11**, 55 (1975).
- <sup>18</sup>J. J. Bara, B. V. Gajič, A. T. Pędziwiatr, and A. Szytuła, *J. Magn. Magn. Mater.* **23**, 149 (1981).
- <sup>19</sup>Hisao Yamamoto, *J. Phys. Soc. Jpn.* **20**, 2164 (1965).
- <sup>20</sup>Yoji Nakamura and Ryoichi Tahara, *J. Phys. Soc. Jpn.* **41**, 459 (1976).
- <sup>21</sup>J. W. Drijver, S. G. Sinnema, and F. Van der Woude, *J. Phys. F* **6**, 2165 (1976).
- <sup>22</sup>O. Massenet and H. Daver, *Solid State Commun.* **21**, 37 (1977).
- <sup>23</sup>G. A. Fateseas, *Phys. Rev. B* **8**, 43 (1973).
- <sup>24</sup>A. R. Miedema and F. Van der Woude, *Physica B+C* **100B**, 145 (1980).
- <sup>25</sup>A. M. van der Kraan and K. H. J. Buschow, *Phys. Rev. B* **27**, 693 (1983).
- <sup>26</sup>L. R. Walker, G. K. Wertheim, and V. Jaccarino, *Phys. Rev. Lett.* **6**, 98 (1968).
- <sup>27</sup>H. H. Hamdeh, B. Fultz, and D. H. Pearson, *Phys. Rev. B* **39**, 11 233 (1989).